Do early diagenetic processes affect the applicability of commonly-used organic matter source tracking tools? An assessment through controlled degradation end-member mixing experiments

Morgane Derrien, Heybin Choi, Emilie Jardé, Kyung-Hoon Shin, Jin Hur

1   # Do early diagenetic processes affect the applicability of

2   # commonly-used organic matter source tracking tools? An

3   # assessment through controlled degradation end-member mixing

4   # experiments

5

6

7   Morgane Derrien[a,*], Heybin Choi[b], Jardé Emilie[c], Kyung-Hoon Shin[b], and Jin Hur[a,*]

8   *[a]Department of Environment and Energy, Sejong University, Seoul 143-747, South Korea*

9   *[b]Department of Environmental Marine Sciences, Hanyang University, Ansan, Gyeonggi do*

10   *15588, South Korea*

11   *[c] University of Rennes 1, CNRS, Géosciences Rennes, UMR 6118, Rennes, France*

12

13

14

16

17

18

19

20   * Corresponding author

21   Tel. +82-2-6935-2634

22   E-Mail: morganederrien@sejong.ac.kr; jinhur@sejong.ac.kr

1

ABSTRACT

In the development of organic matter (OM) source tracking tools, it is critical to validate if (1) the tracers are conservative with source mixing, and (2) they can be conservative under diagenetic processes (e.g., microbial degradation). In this study, these two critical points were rigorously tested for three commonly-used source tracking tools (i.e., absorbance and fluorescence proxies, stable carbon isotopes and lipid biomarkers) via a controlled experiment at laboratory scale. To this end, two end-members (e.g., soil and algae), which represent the most common and contrasted sources of OM to sediments in an aquatic environment, were mixed in different ratios and then incubated under different oxygen conditions (oxic versus anoxic) in the dark at 25°C for 60 days. The initial and final signals of the source tracking tools were analyzed and compared for each mixing ratio. Based on three evaluation criteria concerning the linearity of the relationships, discrimination sensitivity, and conservative mixing behavior, we evaluated the applicability of the tools to trace the sediment organic matter in the aquatic environment. Although most of the source tracking proxies evaluated in this study showed a conservative nature after incubation, there are only a few that demonstrated both conservative behaviors with the sources mixing and under early diagenetic processes. The fluorescence proxies such as the relative distribution of a humic-like component associated with refractory source material (Ex/Em: 220/430nm), modified fluorescence index (YFI), humification index (HIX), and carbon stable isotope ratios were identified to be the most reliable tracers for tracking sedimentary OM sources under early diagenetic processes. This study provides strong insights into the validation of common OM source tracking tools for sediment and a reasonable guideline to select the optimum indices for source discrimination via end-member mixing analysis.

1.INTRODUCTION

Natural organic matter (NOM) is generated by the breakdown and degradation of organisms involving hydrosphere, biosphere, and geosphere through diverse biological, chemical, and physical processes in the natural environment (Sillanpää, 2015). NOM sources are usually classified as allochthonous or autochthonous. Allochthonous OM, which occurs from outside the aquatic environment, consists of terrigenous materials, such as vascular plants, leaves, root exudates, and soils, exported from the upstream catchment into rivers and lakes. By contrast, autochthonous OM, which is produced within water bodies, derives from aquatic biota (e.g., algae, bacteria, plankton, macrophytes, and nekton) (Derrien et al., 2019a; Volkman and Tanoue, 2002). In aquatic systems, sediments represent a large reservoir of nutrients and NOM from both inputs in various proportions (Briand et al., 2015; Fisher et al., 2005; Southwell et al., 2010; Waterson and Canuel, 2008; Zhang et al., 2009). Indeed, sedimentary OM is derived from bacteria or plankton formed in situ, but also receives allochthonous OM from the upstream catchment. Soil OM is a representative allochthonous OM source and it is easily transported into the rivers and ends up in sediments through hydrological processes (van der Meij et al., 2018). Nowadays, terrestrial organic matter input into surface waters is one of the major concerns in the context of the current climate changes as it is observed in polar regions with the release of "dormant" carbon from permafrost (Bischoff et al., 2016; Vonk et al., 2015; Wild et al., 2019). Sediments are also a reactive compartment where diagenetic processes occur inducing changes. The processes may be physical, chemical, and/or biological in nature and may occur at any time

3

69 subsequent to the arrival of a particle at the sediment-water interface (Henrichs, 1992;

70 Kuznetsova et al., 2019; Milliken, 2003). Among the early diagenetic processes, biodegradation

71 plays a key role as it is one of the main processes causing changes in amount, composition and

72 properties of OM in sediment (Arndt et al., 2013; Derrien et al., 2019a; Guenet et al., 2014).

73   Investigating the processes that control the composition of sedimentary OM is crucial for

74 a thorough understanding of OM dynamics and its role in the carbon cycle at a local and global

75 scale (Gordon and Goni, 2003; Pedrosa-Pàmies et al., 2015). Identifying, apportioning and

76 tracking the sources of OM in aquatic systems require robust, reliable and effective source

77 tracking tools. Absorbance and fluorescence proxies, stable carbon isotopes, and lipid

78 biomarkers are the most commonly-used OM source tracking tools in aquatic systems (Aiken,

79 2014; Bianchi and Canuel, 2011; Derrien et al., 2017; Meyers, 1994). These tools have been

80 applied in diverse environments including soils, sediments, pore-water, river, lakes, and oceans

81 for several decades (Amiotte-Suchet et al., 2007; Benner et al., 1997; Derrien et al., 2015; Fichot

82 et al., 2013; Jaffé et al., 2004; Meyers and Ishiwatari, 1993; Toming et al., 2013; Wakeham and

83 Canuel, 1990; Zimmerman and Canuel, 2001; Zsolnay et al., 1999). Although these tools have

84 been used for decades, their applicability and potential limitations have not been rigorously

85 examined yet. Nevertheless, to fully validate their use, two critical points need to be examined:

86 1) conservative behavior with sources mixing, and 2) conservative behavior under early

87 diagenetic processes (e.g., microbial degradation). In our previous study, based on a simple

88 mixing POM end-member experiment, we demonstrated that the conservative behavior of the

89 OM source tracking tools with the mixing source is not obvious and finally raised the question of

90 the reliability of some of the most commonly-used tools (Derrien et al., 2019b). More recently,

91 we also investigated the biodegradation-induced changes in the porewater DOM for different

4

92   sources (Derrien et al., 2019c). The results of the latter study suggested the existence of different

93   pathways of biodegradation with both positive and negative priming effects depending on the

94   sources and the ratio of labile material. All these observations clearly justify the questioning of

95   the applicability to these tools in natural systems and the necessity to test them for both criteria.

96   In this context, we designed a controlled degradation experiment at laboratory scale using

97   organic-rich sediments artificially composed of two contrasting OM end-members (i.e., soil and

98   algae) at known mixing ratios. The incubations were performed under oxic and anoxic conditions

99   in order to reproduce different configurations of natural sediment (Kristensen, 2000). Hence, this

100 study aimed to establish the applicability of 3 commonly-used source tracking tools (i.e.,

101 absorbance and fluorescence proxies, stable carbon isotopes, and lipid biomarkers) during early

102 diagenetic processes in the natural environment. As a result, the specific objectives of this study

103 were (i) to study the influence of oxygen on the degradation-induced changes, and (ii) to

104 examine the conservative/non conservative behaviors of the three source discrimination tools in

105 artificial sediments before and after biodegradation, and (iii) to evaluate the conservative/non

106 conservative behaviors of the three source discrimination tools with sources mixing in the

107 artificial sediments.

108

109 **2. MATERIAL AND METHODS**

110 **2.1. Experimental design of the incubation experiment**

111   Two end-members (i.e., soil and algae), as the major organic sources of sediments, were

112 mixed at soil to algae ratios of 100:0, 75:25, 50:50, 25:75, and 0:100, respectively, on the basis

113 of organic carbon (OC) concentrations, not their masses, after the OC contents of the two end-

114 members were taken into account. Briefly, a topsoil (0-10cm) sample was collected as the soil

5

115 end-member at Bukhansan National Park (37°43'37.0" N 127°00'50.9") in South Korea. A

116 commercial unicellular green alga (*Chlorella vulgaris*), which is commonly found in lakes and

117 ponds in South Korea, was purchased as the algae end-member from Aquanet Co., Ltd. in

118 Gyeongsangnam-do, South Korea. Detailed information on the two end-members can be found

119 in Derrien et al., 2019b.

120   Incubation experiments in oxic and anoxic conditions were performed in pre-washed and

121 pre-combusted (450°C for 4 hours) 125 ml Wheaton® amber glass bottles with Teflon

122 screwcaps. Samples for anoxic incubation were prepared and sampled using sterile Aldrich®

123 AtmosBag two-hand glove bag. A mass (12 g) of the end-member mixture samples were mixed

124 with ultrapure water (Barnstead™ Easypure™ RoDi, Thermo Scientific) at a solid to solution

125 ratio of 1:4 and equilibrated for 48 h in the dark at room temperature after shaking at 100 rpm for

126 one hour. River water from Jungnang river in Seoul (37° 40' 16″N, 127° 04' 47″E) was used as

127 inoculum for microbial incubation. The collected river water sample was first passed through a

128 GF/C (pre-combusted, 1.2 μm pore-sized) and 10 mM of inorganic nutrients (NH_4NO_3 and

129 K_2HPO_4) was added to the filtered river water for sufficient microbial growth. Then, the

130 inoculum solution was covered by aluminum foil to protect the solution from light to avoid the

131 growth of algae and finally kept at room temperature under slow shaking (80 rpm) for 2 days.

132 Prior to incubation, all artificial sediment samples were spiked with 3% (v/v) of the prepared

133 inoculum, and a sufficient amount (1%, v/v) of nutrients (NH_4NO_3 and K_2HPO_4 at 10 mM) was

134 added to each sample to avoid nutrient limitations during the incubation. Finally, the samples in

135 oxic and anoxic conditions were incubated in the dark at 25°C for 60 days (Guenet et al., 2014;

136 Navel et al., 2012). No control was prepared because it required the poisoning of the samples

137 with either mercuric chloride or sodium azide, which are extremely toxic and environmentally

138 harmful and more importantly result in fluorescence quenching (Park and Snyder, 2018;

139 Retelletti Brogi et al., 2019). Samples under oxic conditions were aerated every 3 days under a

140 fume hood in order to minimize the contamination by microorganisms in the air. Samples were

141 sacrificed for sampling on day 0 and day 60, with "day 0" corresponding to the day when the

142 samples were inoculated. The degradation experiments were carried out in duplicate.

143   The sampling was performed according to the following. First, samples were taken from the

144 incubator and the overlying water was carefully removed not to disturb the sediment. The

145 artificial sediment samples were then centrifuged at 5000 rpm for 20 min to remove the

146 porewater. Finally, the porewater-free sediment samples were freeze-dried, ground, and

147 homogenized for further analyses.

148

149 **2.2. Spectroscopic measurements**

150   To investigate the absorbance and fluorescence properties of the artificial sediment, it is

151 necessary to perform an extraction of the OM (e.g., extraction of the dissolved OM from the

152 sedimentary OM). Extraction can be performed with different solvents. According to our

153 previous results comparing common solvent-based OM extraction methods, the water extraction

154 was identified as the preferred extraction method for the application of the spectroscopic tool to

155 POM source discrimination (Derrien et al., 2019b). In this study, the same procedure was used to

156 obtain the water-extractable organic matter (WEOM) of the artificial sediment samples.

157   The dissolved organic carbon (DOC) concentrations were measured using a Shimadzu V-

158 CPH TOC analyzer. The absorption spectra were scanned from 200 to 800 nm at 0.5 nm-interval

159 using an ultraviolet-visible (UV-vis) spectrometer (Shimadzu UV-1300). The fluorescence

160 excitation-emission matrices (EEMs) were obtained with a luminescence spectrometer (Hitachi

161 F7000, Japan) following the procedure previously described by Retelletti Brogi et al. (2019). A

162 total of 82 EEMs were collected for the PARAFAC modeling, and it was processed using

163 MATLAB R2013b (Mathworks, USA) with the drEEM toolbox (Murphy et al., 2013). The

164 validation of the PARAFAC model was made by split-half analysis and percentage of explained

165 variance (>99.5%). By using corrected EEMs, several classical fluorescence indices (e.g.,

166 fluorescence index and modified fluorescence index: FI and YFI, the humification index: HIX,

167 and the index of recent autochthonous contribution BIX) were calculated (Heo et al., 2016;

168 Huguet et al., 2009; Zsolnay et al., 1999). The maximum fluorescence intensities (F_{max}) of the

169 identified PARAFAC components were used to represent their relative abundance (%).

170

171 **2.3. Carbon and nitrogen stable isotope ratio analyses**

172 Before carbon stable isotope analysis, inorganic carbon was removed by 1N HCl

173 treatment, whereas untreated samples were directly used for the nitrogen isotope ratio analysis

174 (Carabel et al., 2006). The total organic carbon (TOC) and the carbon stable isotope ratio ($\delta^{13}C$)

175 were measured using an elemental analyzer that was coupled with an isotope ratio mass

176 spectrometer (EA-IRMS; EuroEA-Isoprime IRMS, GV Instruments, UK). Stable isotope ratios

177 were calculated using the standard d notation:

$$\delta^{13}C(‰) = \left(\left(R_{sample}/R_{Reference} \right) - 1 \right) \times 1000 \qquad (1)$$

178 where R is the corresponding ratio of $^{13}C/^{12}C$. The standard reference material was IAEA-CH-3,

179 Cellulose ($\delta^{13}C$ = -24.724 ± 0.041 (vs VPDB, Vienna Pee Dee Belemnite)). The analytical

180 precision was 0.05‰.

181

182 **2.4. The sterols/stanols analysis**

183   The total lipid fraction of the artificial sediments was extracted with dichloromethane

184   using an accelerated solvent extractor (ASE 200, Dionex). Conditions of the extraction are

185   described in Derrien et al. (2011). The total lipid extract was then fractionated using solid/liquid

186   chromatography (silica column) to isolate the polar fraction. The polar fraction was derivatized

187   with a mixture of N,O-bis-(trimethylsilyl)trifluoroacetamide and trimethylchloro-silane (BSTFA

188   + TMCS, 99/1, v/v, Supelco) after addition of 5α-cholestane (CDN isotope) as an internal

189   standard (IS). Derivatized samples were analyzed by gas chromatography-mass spectrometry

190   (GC–MS) using a Shimadzu QP2010plus equipped with a capillary column (Supelco,

191   60m×0.25mm ID, 0.25 µm film thickness). The temperature of the transfer line was set at 280°C,

192   and molecules were ionized by electron impact using the energy of 70 eV. The temperature of

193   the ionization source was set at 200°C. Samples were injected in splitless mode at 310°C. The

194   oven temperature was programmed from an initial temperature of 200°C (held for 1 min) then

195   rising to 310°C at 15°C/min (held for 35 min). Helium was used as the carrier gas, with a flow

196   rate of 1.0 mL/min. The analyses were made in selective ion monitoring mode (SIM). The

197   compound identification was performed based on the comparison of the retention times and the

198   mass spectra with the available standards or the literature data (Table S1) (Debieu et al., 1992;

199   Derrien et al., 2019b; Harrault et al., 2019). The quantification was achieved with a 5-point

200   internal calibration curve (two series of calibration solutions: 0.1, 0.3, 0.5, 0.7 and 1ppm or 1, 3,

201   5, 7, and 10 ppm) of sterol and stanol standards with a constant IS concentration at 0.5 or 5 ppm,

202   respectively.

203

204   **2.6. Conservative mixing relationship and statistical analyses**

205   In order to assess the applicability of the different source tracking tools during early

206 diagenetic processes, several evaluation criteria were established, which were already presented

207 and used in a previous study (Derrien et al., 2019b). First, the linearity of the measured

208 parameters in artificial sediments was examined with respect to the increasing abundance of one

209 end-member (e.g., soil or algae). The relationship was considered "linear" for a high coefficient

210 of determination $R^2 > 0.8$ and an associated p-value < 0.01. Then, the regression slope of the

211 measured values (Sm) normalized by the standard deviation of the measurement (Sm/SD) was

212 used to evaluate the sensitivity of the source discrimination. A value of the Sm/SD ≥ 0.5 was

213 considered as an acceptable range for the sensitivity regarding the source discrimination relative

214 to the measurement uncertainty. Finally, the deviation from the ideal values for a conservative

215 mixing relationship was estimated in calculating the percent difference (%difference) between

216 the slopes for the measured (Sm) and the predicted (Sp) values. The predicted values were

217 calculated using the pure end member's values and the mixing ratios under a linear conservative

218 mixing assumption (Table S2). A %difference of $< 10\%$ was considered to be an acceptable

219 degree of the deviation for the conservative mixing relationship.

220

221 **3.RESULTS AND DISCUSSION**

222 **3.1. Spectroscopic indices**

223 3.1.1. Identification of different fluorescent components via EEM-PARAFAC

224   Four different components were identified, which included two humic-like components

225 (C1 and C2) and two protein-like components (C3 and C4) (Fig. S1). All the identified

226 components were consistent with those previously reported and/or matched well with the Open

227 Fluor database with similarity scores > 0.95 (Table S3). Component 1 (C1), which had a

10

228 maximum at 220/430 nm (Ex/Em), can be assigned to a typical terrestrial humic-like component

229 (Graeber et al., 2012; Retelletti Brogi et al., 2019b; Yamashita et al., 2010). Component 2 (C2),

230 which exhibited the maxima at 220/547 nm (Ex/Em) can be associated with a humic-like

231 component or aromatic conjugated macromolecular substances of terrestrial origin (Galletti et

232 al., 2019; Osburn et al., 2016b; Wünsch et al., 2017). Component 3 (C3, peaked at 220,265/361

233 nm (Ex/Em)) and component 4 (C4, peaked at 220/309 nm (Ex/Em)) were reported as protein-

234 like substances, namely tryptophan-like and tyrosine-like components, respectively (Cawley et

235 al., 2012; D'Andrilli et al., 2017; Derrien et al., 2019c; Yamashita et al., 2013).

236

237 3.1.2. Changes in the absorbance and fluorescence proxies of the end-members after incubation

238 The original (at 0-day of incubation) spectroscopic characteristics of the end-members for

239 this study were consistent with those reported in our previous study (Derrien et al., 2019b)

240 (Table 1). Briefly, the soil end-member was mainly characterized by a high abundance of both

241 humic-like components, C1 and C2, with the percentages of > 47% and > 34%, respectively. On

242 the contrary, the algae end-member consisted only of the two protein-like components, C3 and

243 C4, in equal proportions. Higher values of $SUVA_{254}$ (> 2 $L.mg^{-1}.m^{-1}$) and HIX (> 15) were

244 observed for the soil end-member corroborating the high content of humic substances (Derrien

245 et al., 2017; Zsolnay et al., 1999) while higher values of YFI (>3.5) and BIX (>1) were for the

246 algae end-member reflecting its allochthonous origin (Heo et al., 2016; Huguet et al., 2009).

247 The biodegradation led to changes in most of the spectroscopic parameters for both end-

248 members (Table 1). Although there were some differences between the two oxygen conditions,

249 these differences were not statistically significant as the p-values were > 0.95 (e.g., 0.95 and 0.99

250 for soil and algae end-members, respectively). After 60 days of incubation, the soil end member

11

251   exhibited a partial (~30%) to complete decrease in the abundance for both protein-like

252   components (C3 and C4). For the main fluorescent components, biodegradation induced a slight

253   depletion of the component C1 (< 10%) while the second humic-like component (C2) became

254   more enriched by 20 to 30 %. Regarding the spectroscopic indices, substantial changes were

255   mainly observed for HIX with an increase of the value from 16.9 ± 0.7 to 21.3 ± 0.2 under oxic

256   conditions. However, the increase was slight under anoxic conditions. These results suggest the

257   initial consumption of labile substances as reflected by the partial to complete consumption of

258   the two protein-like components, and a production of high molecular weight and aromatic

259   substances (C2) through the alteration of existing compounds (C1) and/or the production of new

260   compounds by autotrophic organisms (Derrien et al., 2019a; Hansen et al., 2016; Kinsey et al.,

261   2018).

262   The algae end member also displayed biodegradation-induced changes in the spectroscopic

263   parameters. The most notable change was the decrease in the relative abundance of the C3

264   component (i.e., %C3) changing from 46.0 ± 0.8 to $42.4 \pm 1.1\%$ in parallel to the increase of the

265   %C4 values from 52.5 ± 0.6 to $56.5 \pm 1.1\%$. The two fluorescence indices, FI and YFI, showed

266   an increasing trend over incubation, with highest increasing trend for FI under oxic conditions

267   (0.7 ± 0.0 to 1.0 ± 0.0) and YFI under anoxic conditions (3.6 ± 0.0 to 4.1 ± 0.0). The rest of the

268   indices exhibited little to slight changes in the values specifically under anoxic conditions. For

269   instance, BIX presented an increase of ~20% after incubation under anoxic conditions compared

270   to 3% under oxic conditions. Although the results could be apparently interpreted as the

271   occurrence of a potential effect of the oxygen condition, the t-test demonstrated that these

272   changes were not significant enough (p-values >0.95). These observations suggest that the

273 biodegradation-induced changes in the spectroscopic source indices were less pronounced for the

274 algae end-member than for the soil counterpart.

275

276 3.1.3. Biodegradation-induced deviations from a relationships

277   Biodegradation-induced changes in the absorbance and fluorescence proxies with the

278 increasing of the algal content in the artificial sediments are shown in Figs. 1 and 2. The oxygen

279 condition does not seem to be a critical factor for the biodegradation-induced changes as the

280 results were similar between the oxic and anoxic conditions (p-value of >0.96). The trends of the

281 proxies at 0 day and 60 days of incubation (i.e., %C1, %C2, YFI, HIX, and BIX; Fig. 1 and Fig.

282 2c, d, e) with increasing algal content in the mixture mostly remained the same (p-values > 0.6

283 for each proxy), which demonstrates a minor effect of the degradation on the changing trends of

284 the signals with source mixing. By contrast, deviations between both incubation times were

285 observed for the proxies including %C3, %C4, $SUVA_{254}$, and FI. $SUVA_{254}$ and FI (Fig 1 and Fig

286 2a, b) displayed a deviation after biodegradation along with the increase of the algae fraction

287 except for the mixing ratio soil/algae 25/75. However, for %C3 and %C4, the deviation is the

288 most pronounced at the particular mixing ratio (i.e., 25/75).

289   In order to evaluate the applicability of spectroscopic indices to identify OM sources

290 during early diagenesis, the initial relationships between the absorbance/fluorescence proxies and

291 the abundance of algal content in the mixture were investigated (Table 2) and then compared to

292 the relationship after the biodegradation (Table 3). At 0-day of incubation (Table 2), only %C1,

293 %C2, %C4, and $SUVA_{254}$ satisfied the threshold values of the three evaluation criteria (i.e., R^2

294 with p-value < 0.01, Sm/SD > 0.5, and % difference > 10%) for one (e.g. %C2 and $SUVA_{254}$) or

295 both of the oxygen conditions (e.g. %C1 and %C4). The parameters of YFI and HIX can also be

13

296 suggested as good indices in terms of the relationship linearity as they meet 2 out of the 3 criteria

297 without any effect of the oxygen condition, while %C3 and FI seem to be reliable indices for

298 anoxic and oxic conditions, respectively. BIX does not validate any of the criteria. Among these

299 spectroscopic indices, after incubation, only %C1, YFI and HIX still satisfied all the evaluation

300 criteria for both oxygen conditions after biodegradation except HIX under anoxic condition

301 which did not validate the sensitivity criterion ($S_m/SD = 0.169$) (Table 3). The other indices

302 failed to meet the criteria in terms of linearity, sensitivity and exhibited a higher degree of the

303 deviation from the ideal end-member mixing ratios (i.e., %C3, %C4, $SUVA_{254}$, FI) after

304 microbial degradation. The non-conservative behavior of the latter indices is probably related to

305 the labile characteristic of these compounds (protein-like). From the comparison of all

306 spectroscopic proxies using the evaluation criteria at 0-day and 60-days incubation, it can be

307 concluded that the relative abundance of C1 and the two fluorescence indices, YFI and HIX,

308 represent the optimum fluorescence proxies for the OM source discrimination with varying end-

309 member mixing ratios.

310

311 **3.2. Carbon isotope ratios**

312 3.2.1. Changes for carbon isotope ratios of the end-members after incubation

313   As has been found for the spectroscopic characteristics, the isotope results of the end-

314 members at 0-day of incubation were similar to those reported in our previous study (Derrien et

315 al., 2019b) and in lines with other literature (Pardue et al., 1976; Yu et al., 2015). The values for

316 the soil end-member were -27.2 ± 0.1‰ (oxic) and -26.7 ± 0.1‰ (anoxic), while those of the

317 algae end-member were -11.9 ± 0.0‰ (oxic) and -11.4 ± 0.1‰ (anoxic).

318   After incubation, the values of each end-member remained invariant suggesting no effect

319   of the biodegradation on the carbon isotopic composition. In addition, no significant difference

320   was observed between the two oxygen conditions as the p-values were >0.3 and >0.9 for soil and

321   algae end-members, respectively. These results confirm the chemical stability of the $\delta^{13}C$ to trace

322   the sedimentary OM under the early diagenetic processes irrespective of oxygen presence.

323

324   3.2.2. Biodegradation-induced deviations from end member mixing analysis (EMMA)

325   relationships

326   Biodegradation-induced changes in the $\delta^{13}C$ values of the artificial sediment mixtures

327   with the increase of the algal content are shown in Fig. 3. The variation of the $\delta^{13}C$ values

328   exhibited a linear relationship with the increase of the algal end member fraction both before and

329   after biodegradation (Tables 2 and 3). In addition, the trend of the carbon stable isotope with

330   increasing algal content in the mixture mostly remained the same before and after 60-days of

331   incubation, demonstrating the resistance to isotopic alteration of $\delta^{13}C$ during sedimentary

332   diagenesis. However, a deviation was exceptionally noted for a mixing ratio with an equal

333   proportion of both end-members (soil/algae, 50/50). The decomposition of OM, mediated by a

334   variety of microbial processes, can progressively modify the bulk composition of the organic

335   substrates because different OM fractions do not have the same degradation rate (Lehmann et al.,

336   2002; Meyers, 1994). Such selective losses of certain OM fractions may lead to a diagenetic shift

337   in $\delta^{13}C$ (Benner et al., 1997; Harvey et al., 1995), leaving irreversible changes in the original

338   signature. This is probably what was observed in this present study for the 50/50 artificial

339   sediment mixture. Although the stable isotopes are widely recognized as a reliable and robust

340   tool to trace sediment OM sources and their linear and conservative behavior in a context of

15

341 artificial end-member mixing (Derrien et al., 2019b), their specificity to individual sources might

342 be weakened by early diagenesis of sediments (Bianchi and Canuel, 2011; Xiao and Liu, 2010).

343 Despite this slight deviation, the δ^{13}C tool satisfied the three (and 2 for anoxic condition)

344 established criteria (e.g., linearity, sensitivity, and deviation), evidencing its linear conservative

345 mixing behavior after biodegradation, with the R^2 values ranging from 0.969 (oxic) and 0.898

346 (anoxic) with the p-values of $\leq$ 0.01, %difference of <10% and a sensitivity Sm/SD of 1.431

347 (oxic condition) (Table 3). These results clearly demonstrate the robustness and reliability of the

348 δ^{13}C tool for source discrimination of the sedimentary OM even after diagenetic processes.

349

350 **3.3. Sterols/stanols biomarkers**

351 3.3.1. Changes in the sterol/stanols distributions of the end-members after incubation

352 The original (at 0-day of incubation) biomarker distribution of the end-members for this

353 study was consistent with those reported in our previous study (Derrien et al., 2019b). Briefly,

354 the soil end member was characterized by abundant amounts (> 80%) of terrestrial sterols, such

355 as sitosterol, stigmasterol, and campesterol (Table 1), which agreed with the previous literature

356 (Bouloubassi et al., 1997; Derrien et al., 2011; Volkman, 2005). Fecosterol, a fungi or lichens

357 sterol biomarker (Debieu et al., 1992), sitostanol (i.e., a by-product of sitosterol) and cholesterol,

358 the most ubiquitous sterol (Leeming and Nichols, 1998), contributed <10% of the total

359 sterol/stanol distribution. Unlike the soil end-member, the algae was characterized by a high

360 abundance (>70%) of ergosterol (i.e., a green algae sterol biomarker) and the occurrence of

361 sitosterol and cholesterol, which corresponded to ~18% and ~5% of the sterol compounds in the

362 distribution, respectively.

16

363   After biodegradation, the distribution in sterols/stanols in the end-members remained the

364   same, suggesting no effect of biodegradation such as it was observed for the carbon isotopic

365   composition.   Likewise, no significant difference was observed between the two oxygen

366   conditions with the p-values of > 0.90 for both end-members. These results confirm the chemical

367   stability of the biomarkers to trace the sedimentary OM sources under 60 days of diagenesis

368   dominated by biodegradation.

369

370   3.3.2. Biodegradation-induced deviations from EMMA relationships

371   Biodegradation-induced changes in the distribution of sterol/stanol biomarkers in the

372   artificial sediments with increasing algal content are shown in Fig. 4. In most cases, the oxygen

373   condition does not seem to be a critical factor for the biodegradation-induced changes, which

374   was observed for all the biomarkers (p-value >0.99).   For all the biomarkers, the observed

375   distribution values at all varying algal content between 0-day and 60-days of incubation were the

376   same based on paired t-test (p-value > 0.5). These observations demonstrate the chemical

377   stability of these lipid biomarkers to biodegradation-induced alterations.

378   Regarding the applicability of the lipid biomarker to identify the source of the

379   sedimentary OM during early diagenesis, none of them satisfy the established evaluation criteria

380   either at 0-day or 60-days of incubation (Table 2 and 3).   Surprisingly, the source-specific

381   biomarkers, found only in one of the two end-members (Table 1) such as ergosterol, fecosterol,

382   campesterol, stigmasterol or sitostanol, even did not follow a conservative behavior with sources

383   mixing before biodegradation as the highest R^2 were still < 0.8 with p-values > 0.05. For

384   example, campesterol, presented a R^2 of 0.695 with a p-values of 0.079 and 0.722 (p-

385   value=0.068) in oxic and anoxic conditions, respectively (Table 2). It is noteworthy that

17

386   biodegradation-induces changes on the sitostanol resulted in improved linearity criterion with the

387   R^2 values changing from 0.530 (0.163) to 0.638 (0.105) and 0.544 (0.155) to 0.723 (0.068) for 0-

388   day and 60-days of incubation, respectively and specifically the reduction in the deviation under

389   anoxic condition (i.e., 11.8% to 6.2%). This singular behavior can be related to the nature of the

390   by-products of the biomarker showing a higher sensitivity to microbial alterations (Bull et al.,

391   2002). On the other hand, the incapability of the sterols and stanols lipid biomarker to reflect a

392   conservative behavior with sources mixing was already suggested by previous studies (Derrien et

393   al., 2019b; Shah et al., 2007). Nevertheless, it is noteworthy to observe the conservative behavior

394   of these lipid biomarkers under early diagenetic processes.

395

396   **3.4. Implications for the applicability of the organic matter source tracking tools**

397   In this study, the discrimination capacities of the commonly used source tracking tools

398   during biodegradation were evaluated and compared using artificial sediments with different

399   mixing ratios of two contrasting OM sources. Two modes were observed: (i) conservative

400   behavior in terms of both sources mixing and biodegradation and (ii) single conservative

401   behavior in terms of biodegradation only. The results of this study demonstrated the strong

402   capacity and the robustness of the carbon stable isotope ratios to identify and estimate the source

403   contribution in artificial sediment mixtures under diagenesis processes. Several spectroscopic

404   indices, such as the relative distribution of the specific fluorescent components (i.e., C1: typical

405   terrestrial humic-like component), YFI, and HIX also represent a robust source tracking tools

406   that were applicable for source apportionment to the artificial sediment mixtures samples under

407   the influence of biodegradation. Regrettably, the lipid biomarkers failed in source apportionment

408   in the artificial sediment mixtures. However, they demonstrated a resistance to microbial

18

409 alterations in time. Regarding the oxygen conditions, this study provides, for the first time, clear

410 evidence of little to slight effect on the efficacy of the 3 tested sources tracking tools in artificial

411 sediment mixtures.

412   All of these tools were widely utilized to track and estimate OM sources in various

413 aquatic environments, including rivers, groundwater, lakes, coastal area and oceans (Affouri and

414 Sahraoui, 2017; Derrien et al., 2018; Li et al., 2015; Ogrinc et al., 2005; Osburn et al., 2016a;

415 Toming et al., 2013; Zhang et al., 2017). They were used with the assumption of a conservative

416 mixing behavior and stability under diagenetic processes without firstly evaluating the potential

417 limited applicability. But this study provides strong evidence that the application of these

418 commonly-used tools for OM source tracking could lead to a disruption of the source assignment

419 to a wrong estimation of OM source contribution in the context of early diagenesis. Aside from

420 demonstrating a certain weakness to a complete failure of some of the commonly-used source

421 tracking tools to identify and estimate OM source contribution, this study also raises the question

422 of temporal scale. 60 days of incubation correspond to a short period of time at the diagenesis

423 scale. Therefore, it is reasonable to presume that in higher temporal scale, the limitations of the

424 tools may increase to reach the point where the source tracking tools will not be sustainable

425 anymore, leading to misinterpretations of the biogeochemical processes and dynamics of the OM

426 in specific environments.

427   Experiments carried out under controlled conditions can help in identifying the effects

428 that certain factors have on OM dynamics and properties by excluding any interferences that

429 might exist in real environments (Derrien et al., 2019a). In the present case, we tried to elucidate

430 the combined effect of multiple factors (i.e., microbial degradation, mixing sources ratios and

431 oxygen condition). Although the results of this study provide significant insights for the

19

432 characterization of the OM and more generally for the biogeosciences field, it is necessary to be

433 aware of some limitations of this kind of approach (i.e., a limited number of OM sources (i.e.,

434 soil and algae) and choice of the degradation time). Nevertheless, in this current framework,

435 carbon stable isotope ratios, the relative distribution of refractory material fluorescent

436 component, YFI and HIX indices could be suggested as a reasonable tracer with the most

437 conservative behavior and the highest sensitivity to source discrimination in the period of early

438 diagenesis.

439

440 **4. CONCLUSION**

441   The applicability of three commonly-used source tracking tools (i.e., fluorescence

442 proxies, carbon stable isotope ratios, and lipid biomarkers) was tested on artificial sediments of

443 different mixing ratios of two contrasting OM sources and after biodegradation for both oxygen

444 conditions (i.e., oxic and anoxic). Based on three evaluation criteria concerning the linearity of

445 the relationships, the discrimination sensitivity, and the conservative mixing behavior, the

446 following conclusions can be drawn:

447 • The oxygen condition seems to make a limited contribution to biodegradation-induced

448   changes by comparing initial and final tested properties after 60 days of degradation.

449 • Most of the sources tracking proxies evaluated in this study show a conservative behavior

450   with respect to biodegradation. By contrast, only a few demonstrated a linear relationship

451   with the increasing portion of one end-members in the mixtures.

452 • The fluorescence proxies such as the relative distribution of a humic-like component

453   associated with refractory source material (C1, Ex/Em: 220/430nm), YFI, and HIX

454   indices were found to be reliable proxies for source tracking after biodegradation.

455   • Carbon stable isotope ratios exhibited a linear conservative relationship with varying

456   mixing ratios of end members before and after biodegradation, demonstrating its strong

457   capacity for identifying the source's contribution at any time under diagenesis.

458   • The biomarkers of sterols/stanols did show a conservative nature under biodegradation

459   however they did not present a good linear and conservative behavior with varying

460   mixing ratios of end members.

461   Although these results clearly demonstrate the sensitivity to early diagenesis processes to

462 most of the commonly used sources tracking tools, further studies need to be performed to

463 rigorously evaluate the effects of the incubation time, temperature, sediment depth to fully

464 validate these results.

469

470 **References**

471 Affouri, H., Sahraoui, O., 2017. The sedimentary organic matter from a Lake Ichkeul core (far

472   northern Tunisia): Rock-Eval and biomarker approach. J. African Earth Sci. 129, 248–259.

473   https://doi.org/10.1016/j.jafrearsci.2017.01.017

474 Aiken, G., 2014. Fluorescence and Dissolved Organic Matter, in: Baker, A., Reynolds, D.M.,

475   Lead, J., Coble, P.G., Spencer, R.G.M. (Eds.), Aquatic Organic Matter Fluorescence.

476   Cambridge University Press, Cambridge, pp. 35–74. https://doi.org/DOI:

477   10.1017/CBO9781139045452.005

478   Amiotte-Suchet, P., Linglois, N., Leveque, J., Andreux, F., 2007. 13C composition of dissolved

479   organic carbon in upland forested catchments of the Morvan Mountains (France): Influence

480   of coniferous and deciduous vegetation. J. Hydrol. 335, 354–363.

481   https://doi.org/http://dx.doi.org/10.1016/j.jhydrol.2006.12.002

482   Arndt, S., Jørgensen, B.B., LaRowe, D.E., Middelburg, J.J., Pancost, R.D., Regnier, P., 2013.

483   Quantifying the degradation of organic matter in marine sediments: A review and synthesis.

484   Earth-Science Rev. 123, 53–86. https://doi.org/10.1016/J.EARSCIREV.2013.02.008

485   Benner, R., Biddanda, B., Black, B., McCarthy, M., 1997. Abundance, size distribution, and

486   stable carbon and nitrogen isotopic compositions of marine organic matter isolated by

487   tangential-flow ultrafiltration. Mar. Chem. 57, 243–263.

488   https://doi.org/http://dx.doi.org/10.1016/S0304-4203(97)00013-3

489   Bianchi, T.S., Canuel, E.A., 2011. Chemical Biomarkers in Aquatic Ecosystems. Princeton

490   University Press, Princeton University.

491   Bischoff, J., Sparkes, R.B., Doğrul Selver, A., Spencer, R.G.M., Gustafsson, Ö., Semiletov, I.P.,

492   Dudarev, O. V., Wagner, D., Rivkina, E., van Dongen, B.E., Talbot, H.M., 2016. Source,

493   transport and fate of soil organic matter inferred from microbial biomarker lipids on the

494   East Siberian Arctic Shelf. Biogeosciences 13, 4899–4914. https://doi.org/10.5194/bg-13-

495   4899-2016

496   Bouloubassi, I., Lipiatou, E., Saliot, A., Tolosa, I., Bayona, J.M.M., Albaigés, J., 1997. Carbon

497   sources and cycle in the western Mediterranean—the use of molecular markers to determine

498   the origin of organic matter. Deep Sea Res. Part II Top. Stud. Oceanogr. 44, 781–799.

499   https://doi.org/https://doi.org/10.1016/S0967-0645(96)00094-X

500   Briand, M.J., Bonnet, X., Goiran, C., Guillou, G., Letourneur, Y., 2015. Major Sources of

501   Organic Matter in a Complex Coral Reef Lagoon: Identification from Isotopic Signatures

502   (δ(13)C   and δ(15)N).   PLoS   One   10,   e0131555.

503   https://doi.org/10.1371/journal.pone.0131555

504   Bull, I.D., Lockheart, M.J., Elhmmali, M.M., Roberts, D.J., Evershed, R.P., 2002. The origin of

505   faeces by means of biomarker detection. Environ. Int. 27, 647–654.

506   Carabel, S., Godínez-Domínguez, E., Verísimo, P., Fernández, L., Freire, J., 2006. An

507   assessment of sample processing methods for stable isotope analyses of marine food webs.

508   J.   Exp.   Mar.   Bio.   Ecol.   336,   254–261.

509   https://doi.org/http://dx.doi.org/10.1016/j.jembe.2006.06.001

510   Cawley, K.M., Ding, Y., Fourqurean, J., Jaffé, R., 2012. Characterising the sources and fate of

511   dissolved organic matter in Shark Bay, Australia: a preliminary study using optical

512   properties   and   stable   carbon   isotopes.   Mar.   Freshw.   Res.   63,   1098–1107.

513   https://doi.org/https://doi.org/10.1071/MF12028

514   D'Andrilli, J., Foreman, C.M., Sigl, M., Priscu, J.C., McConnell, J.R., 2017. A 21 000-year

515   record of fluorescent organic matter markers in the WAIS Divide ice core. Clim. Past 13,

516   533–544.

517   Debieu, D., Gall, C., Gredt, M., Bach, J., Malosse, C., Leroux, P., 1992. Ergosterol biosynthesis

518   and its inhibition by fenpropimorph in Fusarium species. Phytochemistry 31, 1223–1233.

519   https://doi.org/https://doi.org/10.1016/0031-9422(92)80265-G

520   Derrien, M., Brogi, S.R., Gonçalves-Araujo, R., Retelletti Brogi, S., Gonçalves-Araujo, R.,

521   2019a. Characterization of aquatic organic matter: Assessment, perspectives and research

522   priorities. Water Res. 163, 114908. https://doi.org/10.1016/J.WATRES.2019.114908

23

523 Derrien, M., Cabrera, F.A., Tavera, N.L.V., Kantún Manzano, C.A., Vizcaino, S.C., 2015.

524   Sources and distribution of organic matter along the Ring of Cenotes, Yucatan, Mexico:

525   Sterol markers and statistical approaches. Sci. Total Environ. 511.

526   https://doi.org/10.1016/j.scitotenv.2014.12.053

527 Derrien, M., Jardé, E., Gruau, G., Pierson-Wickmann, A.-C., 2011. Extreme variability of steroid

528   profiles in cow feces and pig slurries at the regional scale: Implications for the use of

529   steroids to specify fecal pollution sources in waters. J. Agric. Food Chem. 59.

530   https://doi.org/10.1021/jf201040v

531 Derrien, M., Kim, M.S., Ock, G., Hong, S., Cho, J., Shin, K.H.K.-H.K.H., Hur, J., 2018.

532   Estimation of different source contributions to sediment organic matter in an agricultural-

533   forested watershed using end member mixing analyses based on stable isotope ratios and

534   fluorescence spectroscopy. Sci. Total Environ. 618, 569–578.

535   https://doi.org/https://doi.org/10.1016/j.scitotenv.2017.11.067

536 Derrien, M., Shin, K.-H., Hur, J., 2019b. Assessment on applicability of common source tracking

537   tools for particulate organic matter in controlled end member mixing experiments. Sci.

538   Total Environ. 666, 187–196. https://doi.org/10.1016/j.scitotenv.2019.02.258

539 Derrien, M., Shin, K.-H., Hur, J., 2019c. Biodegradation-induced signatures in sediment pore

540   water dissolved organic matter: Implications from artificial sediments composed of two

541   contrasting sources. Sci. Total Environ. 694, 133714.

542 Derrien, M., Yang, L., Hur, J., 2017. Lipid biomarkers and spectroscopic indices for identifying

543   organic matter sources in aquatic environments: A review. Water Res. 112.

544   https://doi.org/10.1016/j.watres.2017.01.023

545 Fichot, C.G., Kaiser, K., Hooker, S.B., Amon, R.M.W., Babin, M., Bélanger, S., Walker, S.A.,

546   Benner, R., 2013. Pan-Arctic distributions of continental runoff in the Arctic Ocean 3, 1053.

547   https://doi.org/10.1038/srep01053http://dharmasastra.live.cf.private.springer.com/articles/sr

548   ep01053#supplementary-information

549   Fisher, M.M., Reddy, K.R., James, R.T., 2005. Internal nutrient loads from sediments in a

550   shallow, subtropical lake. Lake Reserv. Manag. 21, 338–349.

551   https://doi.org/10.1080/07438140509354439

552   Galletti, Y., Gonnelli, M., Retelletti Brogi, S., Vestri, S., Santinelli, C., 2019. DOM dynamics in

553   open waters of the Mediterranean Sea: New insights from optical properties. Deep. Res.

554   Part I Oceanogr. Res. Pap. 144, 95–114. https://doi.org/10.1016/j.dsr.2019.01.007

555   Gordon, E.S., Goni, M.A., 2003. Sources and distribution of terrigenous organic matter delivered

556   by the Atchafalaya River to sediments in the northern Gulf of Mexico. Geochim.

557   Cosmochim. Acta 67, 2359–2375. https://doi.org/10.1016/S0016-7037(02)01412-6

558   Graeber, D., Gelbrecht, J., Pusch, M.T., Anlanger, C., von Schiller, D., 2012. Agriculture has

559   changed the amount and composition of dissolved organic matter in Central European

560   headwater streams. Sci. Total Environ. 438, 435–446.

561   https://doi.org/https://doi.org/10.1016/j.scitotenv.2012.08.087

562   Guenet, B., Danger, M., Harrault, L., Allard, B., Jauset-Alcala, M., Bardoux, G., Benest, D.,

563   Abbadie, L., Lacroix, G., 2014. Fast mineralization of land-born C in inland waters: first

564   experimental evidences of aquatic priming effect. Hydrobiologia 721, 35–44.

565   https://doi.org/10.1007/s10750-013-1635-1

566   Hansen, A.M., Kraus, T.E.C., Pellerin, B.A., Fleck, J.A., Downing, B.D., Bergamaschi, B.A.,

567   2016. Optical properties of dissolved organic matter (DOM): Effects of biological and

568   photolytic degradation. Limnol. Oceanogr. 61, 1015–1032.

569   https://doi.org/10.1002/lno.10270

570   Harrault, L., Milek, K., Jardé, E., Jeanneau, L., Derrien, M., Anderson, D.G., 2019. Faecal

571   biomarkers can distinguish specific mammalian species in modern and past environments.

572   PLoS One 14, e0211119. https://doi.org/10.1371/journal.pone.0211119

573   Harvey, R.H., Tuttle, J.H., Bell, T.J., 1995. Kinetics of phytoplankton decay during simulated

574   sedimentation: Changes in biochemical composition and microbial activity under oxic and

575   anoxic conditions. Geochim. Cosmochim. Acta 59, 3367–3377.

576   https://doi.org/http://dx.doi.org/10.1016/0016-7037(95)00217-N

577   Henrichs, S.M., 1992. Early diagenesis of organic matter in marine sediments: progress and

578   perplexity. Mar. Chem. 39, 119–149. https://doi.org/10.1016/0304-4203(92)90098-U

579   Heo, Y., Kim, D.-H., Lee, H., Lee, D., Her, Namguk, J., Yoon, 2016. A new fluorescence index

580   with a fluorescence excitation-emission matrix for dissolved organic matter (DOM)

581   characterization. Desalin. Water Treat. 57, 20270–20282.

582   https://doi.org/10.1080/19443994.2015.1110719

583   Huguet, A., Vacher, L., Relexans, S., Saubusse, S., Froidefond, J.M., Parlanti, E., 2009.

584   Properties of fluorescent dissolved organic matter in the Gironde Estuary. Org. Geochem.

585   40, 706–719. https://doi.org/https://doi.org/10.1016/j.orggeochem.2009.03.002

586   Jaffé, R., Boyer, J.N., Lu, X., Maie, N., Yang, C., Scully, N.M., Mock, S., 2004. Source

587   characterization of dissolved organic matter in a subtropical mangrove-dominated estuary

588   by fluorescence analysis. Mar. Chem. 84, 195–210.

589   https://doi.org/https://doi.org/10.1016/j.marchem.2003.08.001

590   Kinsey, J.D., Corradino, G., Ziervogel, K., Schnetzer, A., Osburn, C.L., 2018. Formation of

591   Chromophoric Dissolved Organic Matter by Bacterial Degradation of Phytoplankton-

26

592   Derived Aggregates. Front. Mar. Sci. 4, 430. https://doi.org/10.3389/fmars.2017.00430

593 Kristensen, E., 2000. Organic matter diagenesis at the oxic/anoxic interface in coastal marine

594   sediments, with emphasis on the role of burrowing animals. Hydrobiologia 426, 1–24.

595   https://doi.org/10.1023/A:1003980226194

596 Kuznetsova, O. V, Sevastyanov, V.S., Timerbaev, A.R., 2019. What are the current analytical

597   approaches for sediment analysis related to the study of diagenesis? Highlights from 2010

598   to 2018. Talanta 191, 435–442. https://doi.org/https://doi.org/10.1016/j.talanta.2018.08.080

599 Leeming, R., Nichols, P.D., 1998. Determination of the sources and distribution of sewage and

600   pulp-fibre-derived pollution in the Derwent Estuary, Tasmania, using sterol biomarkers.

601   Mar. Freshw. Res. 49, 7–17. https://doi.org/https://doi.org/10.1071/MF95140

602 Lehmann, M.F., Bernasconi, S.M., Barbieri, A., McKenzie, J.A., 2002. Preservation of organic

603   matter and alteration of its carbon and nitrogen isotope composition during simulated and in

604   situ early sedimentary diagenesis. Geochim. Cosmochim. Acta 66, 3573–3584.

605   https://doi.org/http://dx.doi.org/10.1016/S0016-7037(02)00968-7

606 Li, P., Chen, L., Zhang, W., Huang, Q., 2015. Spatiotemporal Distribution, Sources, and

607   Photobleaching Imprint of Dissolved Organic Matter in the Yangtze Estuary and Its

608   Adjacent Sea Using Fluorescence and Parallel Factor Analysis. PLoS One 10, e0130852.

609   https://doi.org/10.1371/journal.pone.0130852

610 Meyers, P.A., 1994. Preservation of elemental and isotopic source identification of sedimentary

611   organic matter. Chem. Geol. 114, 289–302. https://doi.org/http://dx.doi.org/10.1016/0009-

612   2541(94)90059-0

613 Meyers, P.A., Ishiwatari, R., 1993. Lacustrine organic geochemistry—an overview of indicators

614   of organic matter sources and diagenesis in lake sediments. Org. Geochem. 20, 867–900.

615   https://doi.org/http://dx.doi.org/10.1016/0146-6380(93)90100-P

616   Milliken, K.L., 2003. Late Diagenesis and Mass Transfer in Sandstone–Shale Sequences.

617   Treatise on Geochemistry 159–190. https://doi.org/10.1016/B0-08-043751-6/07091-2

618   Murphy, K.R., Stedmon, C.A., Graeber, D., Bro, R., 2013. Fluorescence spectroscopy and multi-

619   way   techniques.   PARAFAC.   Anal.   Methods   5,   6557–6566.

620   https://doi.org/10.1039/C3AY41160E

621   Navel, S., Mermillod-Blondin, F., Montuelle, B., Chauvet, E., Marmonier, P., 2012. Sedimentary

622   context controls the influence of ecosystem engineering by bioturbators on microbial

623   processes in river sediments. Oikos 121, 1134–1144. https://doi.org/doi:10.1111/j.1600-

624   0706.2011.19742.x

625   Ogrinc, N., Fontolan, G., Faganeli, J., Covelli, S., 2005. Carbon and nitrogen isotope

626   compositions of organic matter in coastal marine sediments (the Gulf of Trieste, N Adriatic

627   Sea): indicators of sources and preservation. Mar. Chem. 95, 163–181.

628   https://doi.org/http://dx.doi.org/10.1016/j.marchem.2004.09.003

629   Osburn, C.L., Boyd, T.J., Montgomery, M.T., Bianchi, T.S., Coffin, R.B., Paerl, H.W., 2016a.

630   Optical Proxies for Terrestrial Dissolved Organic Matter in Estuaries and Coastal Waters.

631   Front. Mar. Sci. 2. https://doi.org/10.3389/fmars.2015.00127

632   Osburn, C.L., Handsel, L.T., Peierls, B.L., Paerl, H.W., 2016b. Predicting Sources of Dissolved

633   Organic Nitrogen to an Estuary from an Agro-Urban Coastal Watershed. Environ. Sci.

634   Technol. 50, 8473–8484. https://doi.org/10.1021/acs.est.6b00053

635   Pardue, J.W., Scalan, R.S., Van Baalen, C., Parker, P.L., 1976. Maximum carbon isotope

636   fractionation in photosynthesis by blue-green algae and a green alga. Geochim. Cosmochim.

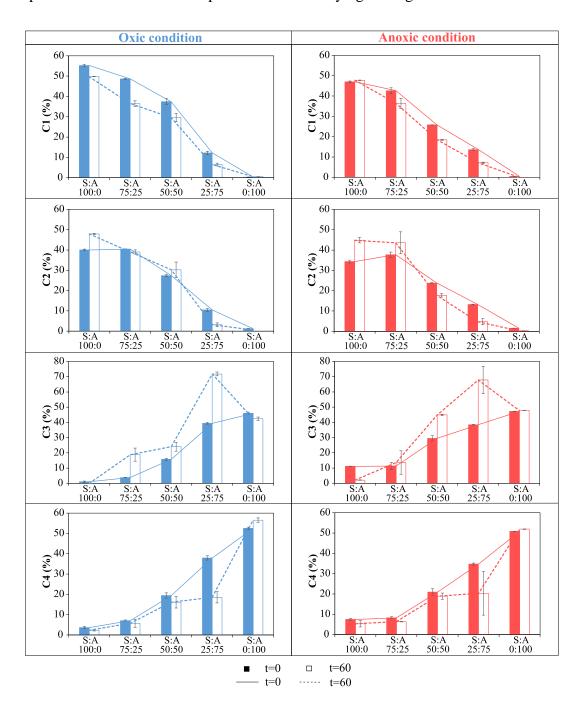637   Acta 40, 309–312. https://doi.org/https://doi.org/10.1016/0016-7037(76)90208-8

638   Park, M., Snyder, S.A., 2018. Sample handling and data processing for fluorescent excitation-

639   emission matrix (EEM) of dissolved organic matter (DOM). Chemosphere 193, 530–537.

640   https://doi.org/https://doi.org/10.1016/j.chemosphere.2017.11.069

641   Pedrosa-Pàmies, R., Parinos, C., Sanchez-Vidal, A., Gogou, A., Calafat, A., Canals, M.,

642   Bouloubassi, I., Lampadariou, N., 2015. Composition and sources of sedimentary organic

643   matter in the deep eastern Mediterranean Sea. Biogeosciences 12, 7379–7402.

644   https://doi.org/10.5194/bg-12-7379-2015

645   Retelletti Brogi, S., Derrien, M., Hur, J., 2019a. In-Depth Assessment of the Effect of Sodium

646   Azide on the Optical Properties of Dissolved Organic Matter. J. Fluoresc. 1–9.

647   https://doi.org/10.1007/s10895-019-02398-w

648   Retelletti Brogi, S., Kim, J.-H., Ryu, J.-S., Jin, Y.K., Lee, Y.K., Hur, J., 2019b. Exploring

649   sediment porewater dissolved organic matter (DOM) in a mud volcano: Clues of a

650   thermogenic DOM source from fluorescence spectroscopy. Mar. Chem.

651   https://doi.org/10.1016/J.MARCHEM.2019.03.009

652   Shah, V.G.., Dunstan, R.H.., Geary, P.M.., Coombes, P.., Roberts, T.K.., Von Nagy-Felsobuki,

653   E., 2007. Evaluating potential applications of faecal sterols in distinguishing sources of

654   faecal contamination from mixed faecal samples. Water Res. 41, 3691–3700.

655   https://doi.org/10.1016/j.watres.2007.04.006

656   Sillanpää, M., 2015. Natural Organic Matter in Water: Characterization and Treatment Methods,

657   Natural Organic Matter in Water: Characterization and Treatment Methods. Elsevier Inc.

658   https://doi.org/10.1016/C2013-0-19213-6

659   Southwell, M.W., Kieber, R.J., Mead, R.N., Avery, G.B., Skrabal, S.A., 2010. Effects of sunlight

660   on the production of dissolved organic and inorganic nutrients from resuspended sediments.

661 Biogeochemistry 98, 115–126. https://doi.org/10.1007/s10533-009-9380-2

662 Toming, K., Tuvikene, L., Vilbaste, S., Agasild, H., Viik, M., Kisand, A., Feldmann, T., Martma,

663 T., Jones, R.I., Nõges, T., 2013. Contributions of autochthonous and allochthonous sources

664 to dissolved organic matter in a large, shallow, eutrophic lake with a highly calcareous

665 catchment. Limnol. Oceanogr. 58, 1259–1270. https://doi.org/10.4319/lo.2013.58.4.1259

666 van der Meij, W.M., Temme, A.J.A.M., Lin, H.S., Gerke, H.H., Sommer, M., 2018. On the role

667 of hydrologic processes in soil and landscape evolution modeling: concepts, complications

668 and partial solutions. Earth-Science Rev. https://doi.org/10.1016/j.earscirev.2018.09.001

669 Volkman, J.K., 2005. Sterols and other triterpenoids: source specificity and evolution of

670 biosynthetic pathways. Org. Geochem. 36, 139–159.

671 https://doi.org/10.1016/J.ORGGEOCHEM.2004.06.013

672 Volkman, J.K., Tanoue, E., 2002. Chemical and Biological Studies of Particulate Organic Matter

673 in the Ocean. J. Oceanogr. 58, 265–279. https://doi.org/10.1023/a:1015809708632

674 Vonk, J.E., Tank, S.E., Mann, P.J., Spencer, R.G.M., Treat, C.C., Striegl, R.G., Abbott, B.W.,

675 Wickland, K.P., 2015. Biodegradability of dissolved organic carbon in permafrost soils and

676 aquatic systems: a meta-analysis. Biogeosciences 12, 6915–6930.

677 https://doi.org/10.5194/bg-12-6915-2015

678 Wakeham, S.G., Canuel, E.A., 1990. Fatty acids and sterols of particulate matter in a brackish

679 and seasonally anoxic coastal salt pond. Org. Geochem. 16, 703–713.

680 https://doi.org/http://dx.doi.org/10.1016/0146-6380(90)90111-C

681 Waterson, E.J., Canuel, E.A., 2008. Sources of sedimentary organic matter in the Mississippi

682 River and adjacent Gulf of Mexico as revealed by lipid biomarker and $\delta13CTOC$ analyses.
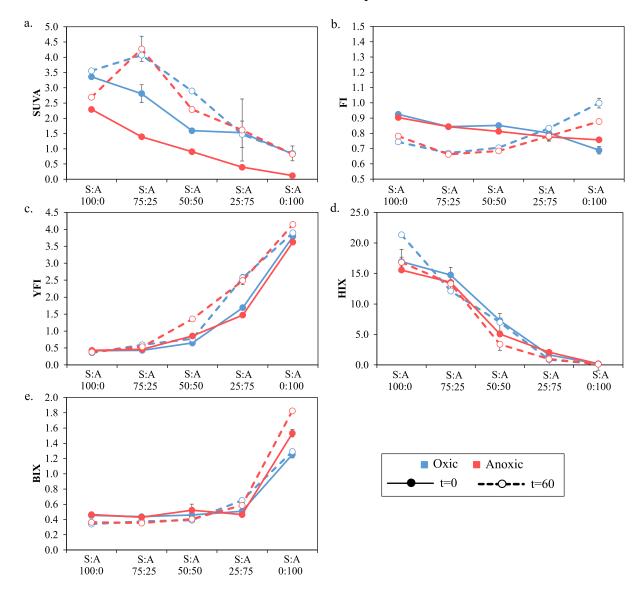
683 Org. Geochem. 39, 422–439.

684   https://doi.org/https://doi.org/10.1016/j.orggeochem.2008.01.011

685   Wild, B., Andersson, A., Bröder, L., Vonk, J., Hugelius, G., McClelland, J.W., Song, W.,

686   Raymond, P.A., Gustafsson, Ö., 2019. Rivers across the Siberian Arctic unearth the patterns

687   of carbon release from thawing permafrost. Proc. Natl. Acad. Sci. U. S. A. 116, 10280–

688   10285. https://doi.org/10.1073/pnas.1811797116

689   Wünsch, U.J., Murphy, K.R., Stedmon, C.A., 2017. The One-Sample PARAFAC Approach

690   Reveals Molecular Size Distributions of Fluorescent Components in Dissolved Organic

691   Matter. Environ. Sci. Technol. https://doi.org/10.1021/acs.est.7b03260

692   Xiao, H.-Y., Liu, C.-Q., 2010. Identifying organic matter provenance in sediments using isotopic

693   ratios in an urban river. Geochem. J. 44, 181–187. https://doi.org/10.2343/geochemj.1.0059

694   Yamashita, Y., Boyer, J.N., Jaffé, R., 2013. Evaluating the distribution of terrestrial dissolved

695   organic matter in a complex coastal ecosystem using fluorescence spectroscopy. Cont. Shelf

696   Res. 66, 136–144. https://doi.org/http://dx.doi.org/10.1016/j.csr.2013.06.010

697   Yamashita, Y., Maie, N., Briceño, H., Jaffé, R., 2010. Optical characterization of dissolved

698   organic matter in tropical rivers of the Guayana Shield, Venezuela. J. Geophys. Res.

699   Biogeosciences 115, n/a-n/a. https://doi.org/10.1029/2009JG000987

700   Yu, Z.T., Wang, X.J., Zhang, E.L., Zhao, C.Y., Liu, X.Q., 2015. Spatial distribution and sources

701   of organic carbon in the surface sediment of Bosten Lake, China. Biogeosciences 12, 6605–

702   6615. https://doi.org/10.5194/bg-12-6605-2015

703   Zhang, L., Yin, K., Wang, L., Chen, F., Zhang, D., Yang, Y., 2009. The sources and

704   accumulation rate of sedimentary organic matter in the Pearl River Estuary and adjacent

705   coastal area, Southern China. Estuar. Coast. Shelf Sci. 85, 190–196.

706   https://doi.org/10.1016/j.ecss.2009.07.035

707   Zhang, Y., Su, Y., Liu, Z., Yu, J., Jin, M., 2017. Lipid biomarker evidence for determining the

708   origin and distribution of organic matter in surface sediments of Lake Taihu, Eastern China.

709   Ecol. Indic. 77, 397–408. https://doi.org/https://doi.org/10.1016/j.ecolind.2017.02.031

710   Zimmerman, A.R., Canuel, E.A., 2001. Bulk Organic Matter and Lipid Biomarker Composition

711   of Chesapeake Bay Surficial Sediments as Indicators of Environmental Processes. Estuar.

712   Coast. Shelf Sci. 53, 319–341. https://doi.org/http://dx.doi.org/10.1006/ecss.2001.0815

713   Zsolnay, A., Baigar, E., Jimenez, M., Steinweg, B., Saccomandi, F., 1999. Differentiating with

714   fluorescence spectroscopy the sources of dissolved organic matter in soils subjected to

715   drying. Chemosphere 38, 45–50. https://doi.org/http://dx.doi.org/10.1016/S0045-

716   6535(98)00166-0
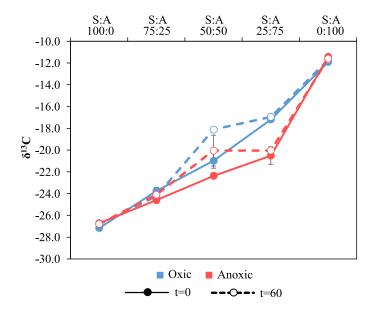
717

Figure 1. Relative abundances (%) of the four different fluorescent components (C1–C4) in the artificial sediments at five different mixing ratios of two end-members (i.e., soil and algae) under oxic and anoxic conditions at the incubation time of 0 and 60 days. The lines and dashed lines represent the evolution of the parameters with varying mixing ratios of the two end-members.

Figure 2. Values of the absorbance and fluorescent indices SUVA (a), FI (b), YFI (c), HIX (d), and BIX (e) in the artificial sediments at five different mixing ratios of two end-members (i.e., soil and algae) under oxic and anoxic conditions at the incubation time of 0 and 60 days. The blue color is used for the data of oxic conditions while pink color for those of anoxic conditions.

Figure 3. Values of the carbon stable isotopes in the artificial sediments at five different mixing ratios of two end-members (i.e., soil and algae) under oxic and anoxic conditions at the incubation time of 0 and 60 days. The blue color is used for the data of oxic conditions while pink color for those of anoxic conditions.

Figure 4. Relative abundances (%) of the seven sterols/stanols in the artificial sediments at five different mixing ratios of two end-members (i.e., soil and algae) under oxic and anoxic conditions at the incubation time of 0 and 60 days. The lines and dashed lines represent the evolution of the parameters with varying mixing ratios of the two end-members.
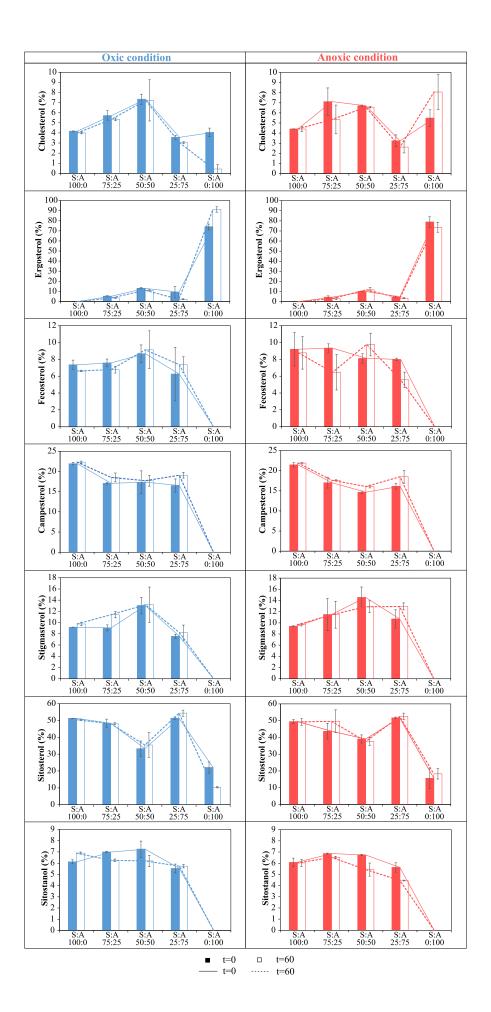
Oxic condition — Anoxic condition

Cholesterol (%), Ergosterol (%), Fecosterol (%), Campesterol (%), Stigmasterol (%), Sitosterol (%), Sitostanol (%) plotted against S:A ratios (100:0, 75:25, 50:50, 25:75, 0:100) for both oxic (blue) and anoxic (red) conditions.

■ t=0   □ t=60
— t=0   ---- t=60

Table 1. The relative changes of the 4 identified components (%) and the spectroscopic indices, the carbon stable isotopic ratios (‰) and the distribution in the sterols/stanols in the artificial sediment of the two end-members before versus after incubation under oxic and anoxic conditions (average values ± standard deviation).

		Soil end-member				Algae end-member			
		Oxic		Anoxic		Oxic		Anoxic	
		0 day-incubation	60 days-incubation	0 day-incubation	60 days-incubation	0 day-incubation	60 days-incubation	0 day-incubation	60 days-incubation
Absorbance and fluorescence proxies	C1 (%)	55.2 ± 0.6	49.8 ± 0.1	47.0 ± 0.4	47.7 ± 0.1	0.3 ± 0.1	0.5 ± 0.0	0.5 ± 0.0	0.0 ± 0.0
	C2 (%)	40.0 ± 0.4	47.9 ± 0.3	34.4 ± 0.7	44.8 ± 1.3	1.2 ± 0.1	0.6 ± 0.0	1.5 ± 0.0	0.2 ± 0.0
	C3 (%)	1.1 ± 0.5	0.0 ± 0.0	11.2 ± 0.1	2.1 ± 0.1	46.0 ± 0.8	42.4 ± 1.1	47.2 ± 0.1	47.8 ± 0.1
	C4 (%)	3.7 ± 0.5	2.3 ± 0.3	7.5 ± 0.4	5.3 ± 1.6	52.5 ± 0.6	56.5 ± 1.1	50.8 ± 0.1	51.9 ± 0.1
	$SUVA_{254}$ (L.mg^{-1}.m^{-1})	3.4 ± 0.1	3.6 ± 0.1	2.3 ± 0.0	2.7 ± 0.1	0.8 ± 0.1	0.8 ± 0.2	0.1 ± 0.0	0.8 ± 0.0
	FI	0.9 ± 0.0	0.7 ± 0.0	0.9 ± 0.0	0.8 ± 0.0	0.7 ± 0.0	1.0 ± 0.0	0.8 ± 0.0	0.9 ± 0.0
	YFI	0.4 ± 0.0	0.4 ± 0.0	0.4 ± 0.0	0.4 ± 0.0	3.8 ± 0.0	3.9 ± 0.0	3.6 ± 0.0	4.1 ± 0.0
	HIX	16.9 ± 0.7	21.3 ± 0.2	15.6 ± 0.4	16.8 ± 2.1	0.2 ± 0.0	0.2 ± 0.0	0.2 ± 0.0	0.1 ± 0.0
	BIX	0.5 ± 0.0	0.3 ± 0.0	0.5 ± 0.0	0.4 ± 0.0	1.3 ± 0.0	1.3 ± 0.0	1.5 ± 0.0	1.8 ± 0.0
Isotopes	$\delta^{13}C$ (‰)	-27.2 ± 0.1	-26.8 ± 0.1	-26.7 ± 0.1	-26.8 ± 0.1	-11.9 ± 0.0	-11.7 ± 0.0	-11.4 ± 0.1	-11.6 ± 0.1
Sterols/stanols	Cholesterol (%)	4.2 ± 0.0	4.0 ± 0.1	4.4 ± 0.0	4.4 ± 0.2	4.1 ± 0.4	0.4 ± 0.4	5.5 ± 0.8	8.1 ± 1.8
	Ergosterol (%)	0.0 ± 0.0	0.0 ± 0.0	0.0 ± 0.0	0.0 ± 0.0	73.9 ± 2.9	91.1 ± 2.7	78.9 ± 5.2	73.6 ± 4.9
	Fecosterol (%)	7.4 ± 0.6	6.6 ± 0.1	9.2 ± 2.0	8.8 ± 1.9	0.0 ± 0.0	0.0 ± 0.0	0.0 ± 0.0	0.0 ± 0.0
	Campesterol (%)	21.9 ± 0.3	22.3 ± 0.3	21.5 ± 0.5	21.9 ± 0.1	0.0 ± 0.0	0.0 ± 0.0	0.0 ± 0.0	0.0 ± 0.0
	Stigmasterol (%)	9.2 ± 0.0	9.8 ± 0.3	9.4 ± 0.0	9.7 ± 0.2	0.0 ± 0.0	0.0 ± 0.0	0.0 ± 0.0	0.0 ± 0.0
	Sitosterol (%)	51.3 ± 0.1	50.4 ± 0.5	49.1 ± 1.1	49.2 ± 2.0	22.1 ± 3.3	10.3 ± 0.4	15.6 ± 6.0	18.3 ± 3.1
	Sitostanol (%)	6.1 ± 0.2	6.9 ± 0.1	6.1 ± 0.4	6.0 ± 0.3	0.0 ± 0.0	0.0 ± 0.0	0.0 ± 0.0	0.0 ± 0.0

Table 2. The evaluation of selected source discrimination indices in the relationships with increasing algal carbon fraction (% Algae) of the artificial sediments at 0-day incubation.

Parameters	Oxygen condition	Tendency	Relationship type[a]	R^2 (p-value)	S_m[b]	S_m/SD[c]	S_p[d]	% difference[e]	Applicability[f]
Extractable OM									
C1 (%)	Oxic	↓	Linear	**0.958 (<0.01)**	0.585	**0.905**	0.550	**6.5**	**OOO**
	Anoxic	↓	Linear	**0.979 (<0.01)**	0.488	**0.992**	0.465	**4.9**	**OOO**
C2 (%)	Oxic	↓	Linear	**0.933 (<0.01)**	0.430	**1.159**	0.388	10.9	**OOX**
	Anoxic	↓	Linear	**0.904 (<0.01)**	0.361	**0.752**	0.328	**9.9**	**OOO**
C3 (%)	Oxic	↑	Linear	**0.935 (<0.01)**	0.501	**0.917**	0.449	11.7	**OOX**
	Anoxic	↑	Linear	**0.946 (<0.01)**	0.397	0.443	0.360	10.1	OXX
C4 (%)	Oxic	↑	Linear	**0.956 (<0.01)**	0.514	**0.668**	0.488	**5.3**	**OOO**
	Anoxic	↑	Linear	**0.939 (<0.01)**	0.452	**0.713**	0.433	**4.4**	**OOO**
SUVA254 (L.mg^{-1}.m^{-1})	Oxic	↓	Linear	**0.944 (<0.01)**	0.025	0.258	0.025	0.3	OXX
	Anoxic	↓	Linear	**0.961 (<0.01)**	0.021	**1.433**	0.022	**1.6**	**OOO**
FI	Oxic	↓	Linear	**0.877** (0.019)	0.002	0.290	0.002	13.0	OXX
	Anoxic	↓	Linear	**0.964 (<0.01)**	0.001	0.137	0.001	**1.5**	**OXO**
YFI	Oxic	↑	Nonlinear	0.775 (0.049)	0.032	**1.419**	0.034	**5.0**	**XOO**
	Anoxic	↑	Nonlinear	0.774 (0.049)	0.030	**3.006**	0.032	**7.4**	**XOO**
HIX	Oxic	↓	Linear	**0.956 (<0.01)**	0.186	**0.551**	0.168	11.3	**OOX**
	Anoxic	↓	Linear	**0.937 (<0.01)**	0.169	0.471	0.154	**9.9**	**OXO**
BIX	Oxic	↑	Nonlinear	0.558 (0.147)	0.007	0.361	0.008	16.5	XXX
	Anoxic	↑	Nonlinear	0.519 (0.170)	0.009	0.262	0.011	18.7	XXX
$\delta^{13}C$ (‰)	Oxic	↑	Linear	**0.985 (<0.01)**	0.148	**0.660**	0.153	**2.8**	**OOO**
	Anoxic	↑	Linear	**0.863** (0.023)	0.139	0.481	0.153	**9.3**	**OXO**
Cholesterol (%)	Oxic	↓	Nonlinear	0.059 (0.694)	0.010	0.029	0.001	726.5	XXX
	Anoxic	↓	Nonlinear	0.028 (0.787)	0.007	0.012	0.011	163.2	XXX
Ergosterol (%)	Oxic	↑	Nonlinear	0.625 (0.111)	0.607	0.299	0.739	17.8	XXX
	Anoxic	↑	Nonlinear	0.562 (0.144)	0.632	0.418	0.789	19.9	XXX
Fecosterol (%)	Oxic	↓	Nonlinear	0.541 (0.157)	0.064	0.061	0.074	12.8	XXX
	Anoxic	↓	Nonlinear	0.635 (0.107)	0.079	0.123	0.092	14.1	XXX
Campesterol (%)	Oxic	↓	Nonlinear	0.695 (0.079)	0.178	0.179	0.219	19.0	XXX
	Anoxic	↓	Nonlinear	0.722 (0.068)	0.175	0.300	0.215	18.4	XXX

Stigmasterol (%)	Oxic	↓	Nonlinear	0.429 (0.230)	0.079	0.167	0.092	13.5	XXX
	Anoxic	↓	Nonlinear	0.319 (0.321)	0.079	0.061	0.094	16.6	XXX
Sitosterol (%)	Oxic	↓	Nonlinear	0.447 (0.217)	0.221	0.101	0.292	24.1	XXX
	Anoxic	↓	Nonlinear	0.428 (0.231)	0.239	0.080	0.338	29.4	XXX
Sitostanol (%)	Oxic	↓	Nonlinear	0.530 (0.163)	0.055	0.200	0.061	10.4	XXX
	Anoxic	↓	Nonlinear	0.544 (0.155)	0.054	0.296	0.061	11.8	XXX

[a]: The relationship is considered linear for $R^2 > 0.8$ with a *p*-value < 0.01.

[b]: The absolute value of the regression slope for the measured values.

[c]: The absolute value of the regression slope for the measured values divided by the average standard deviation of the measurement. A value of the S_m/SD superior to 1.0 was considered as an acceptable sensitivity in the source discrimination relative to the measurement uncertainty

[d]: The absolute value of the regression slope for the predicted values (e.g., data presented in Table S2).

[e]: The difference (%) between the slope of the measured and predicted values. A difference of $< 10\%$ is considered an acceptable deviation. The value of 10% was arbitrarily chosen by the authors.

[f]: The applicability is evaluated via the criteria based on R^2, S_m/SD, and % difference. O means the value of the standard respect the critical value while X the indices failed (e.g., Critical values for R^2 and an associated p-value of R^2, S_m/SD and % difference are > 0.8 and < 0.01, > 0.5, and $< 10\%$, respectively).

Table 3. The evaluation of selected source discrimination indices in the relationships with increasing algal carbon fraction (% Algae) of the artificial sediments at 60-days incubation.

Parameters	Oxygen condition	Tendency	Relationship type[a]	R^2 (p-value)	S_m[b]	S_m/SD[c]	S_p[d]	% difference[e]	Applicability[f]
Extractable OM									
C1 (%)	Oxic	↓	Linear	**0.967 (<0.01)**	0.514	**0.614**	0.493	**4.4**	**OOO**
	Anoxic	↓	Linear	**0.980 (<0.01)**	0.499	**0.795**	0.477	**4.5**	**OOO**
C2 (%)	Oxic	↓	Linear	**0.937 (<0.01)**	0.522	0.439	0.473	10.3	OXX
	Anoxic	↓	Linear	**0.922 (<0.01)**	0.512	0.281	0.446	14.9	OXX
C3 (%)	Oxic	↑	Linear	0.643 (0.103)	0.551	0.284	0.424	30.0	XXX
	Anoxic	↑	Linear	0.737 (0.063)	0.582	0.168	0.457	27.5	XXX
C4 (%)	Oxic	↑	Linear	0.787 (0.045)	0.485	0.268	0.542	10.5	XXX
	Anoxic	↑	Linear	**0.809 (0.038)**	0.429	0.152	0.466	**8.0**	**OXO**
SUVA254 (L.mg^{-1}.m^{-1})	Oxic	↓	Linear	**0.856 (0.024)**	0.032	0.192	0.027	18.4	OXX
	Anoxic	↓	Nonlinear	0.611 (0.118)	0.026	0.080	0.019	36.9	XXX
FI	Oxic	↑	Nonlinear	0.654 (0.097)	0.003	0.200	0.003	**5.7**	XXO
	Anoxic	↑	Nonlinear	0.321 (0.319)	0.001	0.112	0.001	29.8	XXX
YFI	Oxic	↑	Linear	**0.867 (0.021)**	0.036	**0.682**	0.035	**2.3**	**OOO**
	Anoxic	↑	Linear	**0.919 (<0.01)**	0.038	**0.688**	0.038	**0.8**	**OOO**
HIX	Oxic	↓	Linear	**0.934 (<0.01)**	0.214	**0.542**	0.212	**1.3**	**OOO**
	Anoxic	↓	Linear	**0.898 (0.014)**	0.183	0.169	0.167	**9.5**	**OXO**
BIX	Oxic	↑	Nonlinear	0.739 (0.062)	0.009	**0.534**	0.010	**8.5**	XOX
	Anoxic	↑	Nonlinear	0.622 (0.113)	0.013	**1.202**	0.015	13.6	XOX
δ^{13}C (‰)	Oxic	↑	Linear	**0.969 (<0.01)**	0.150	**1.431**	0.151	**0.7**	**OOO**
	Anoxic	↑	Nonlinear	**0.898 (0.014)**	0.138	0.274	0.152	**9.3**	**OXO**
Cholesterol (%)	Oxic	↓	Nonlinear	0.346 (0.297)	0.038	0.068	0.036	**5.8**	XXO
	Anoxic	↓	Nonlinear	0.123 (0.563)	0.018	0.022	0.037	49.8	XXX
Ergosterol (%)	Oxic	↑	Nonlinear	0.536 (0.160)	0.724	**0.835**	0.911	20.6	XOX
	Anoxic	↑	Nonlinear	0.560 (0.146)	0.591	0.335	0.736	19.8	XXX
Fecosterol (%)	Oxic	↓	Nonlinear	0.328 (0.313)	0.051	0.069	0.066	23.7	XXX
	Anoxic	↓	Nonlinear	0.591 (0.129)	0.074	0.059	0.088	16.0	XXX
Campesterol (%)	Oxic	↓	Nonlinear	0.620 (0.114)	0.176	0.262	0.223	21.0	XXX
	Anoxic	↓	Nonlinear	0.630 (0.109)	0.172	0.392	0.219	21.6	XXX

Stigmasterol (%)	Oxic	↓	Nonlinear	0.495 (0.185)	0.091	0.084	0.098	**6.9**	XXO
	Anoxic	↓	Nonlinear	0.272 (0.367)	0.071	0.082	0.097	26.2	XXX
Sitosterol (%)	Oxic	↓	Nonlinear	0.427 (0.232)	0.296	0.140	0.401	26.3	XXX
	Anoxic	↓	Nonlinear	0.434 (0.227)	0.236	0.073	0.309	23.8	XXX
Sitostanol (%)	Oxic	↓	Nonlinear	0.638 (0.105)	0.057	0.328	0.069	17.0	XXX
	Anoxic	↓	Nonlinear	0.723 (0.068)	0.056	0.278	0.060	**6.2**	XXO

[a]: The relationship is considered linear for $R^2 > 0.8$ with a p-value < 0.01.

[b]: The absolute value of the regression slope for the measured values.

[c]: The absolute value of the regression slope for the measured values divided by the average standard deviation of the measurement. A value of the S_m/SD superior to 1.0 was considered as an acceptable sensitivity in the source discrimination relative to the measurement uncertainty

[d]: The absolute value of the regression slope for the predicted values (e.g., data presented in Table S2).

[e]: The difference (%) between the slope of the measured and predicted values. A difference of $< 10\%$ is considered an acceptable deviation.

[f]: The applicability is evaluated via the criteria based on R^2, S_m/SD, and % difference. O means the value of the standard respect the critical value while X the indices failed (e.g., Critical values for R^2 and an associated p-value of R^2, S_m/SD and % difference are > 0.8 and < 0.01, > 0.5, and $< 10\%$, respectively).